PHYTOTHERAPY RESEARCH
Phytother. Res. **27**: 484–492 (2013)
Published online 24 May 2012 in Wiley Online Library
(wileyonlinelibrary.com) **DOI**: 10.1002/ptr.4743

The Effects of an Antiosteoporosis Herbal Formula Containing Epimedii Herba, Ligustri Lucidi Fructus and Psoraleae Fructus on Density and Structure of Rat Long Bones Under Tail-Suspension, and its Mechanisms of Action

Wing-Sum Siu,[1,2,3] Hing-Lok Wong,[4] Ching-Po Lau,[1,2] Wai-Ting Shum,[1,2] Chun-Wai Wong,[1,2] Si Gao,[1,2] Kwok-Pui Fung,[1,2,5] Clara Bik-San Lau,[1,2] Leung-Kim Hung,[3] Chun-Hay Ko[1,2]* and Ping-Chung Leung[1,2,3,4]*

[1]Institute of Chinese Medicine, The Chinese University of Hong Kong, Shatin, New Territories, Hong Kong
[2]State Key Laboratory of Phytochemistry and Plant Resources in West China, The Chinese University of Hong Kong, Shatin, New Territories, Hong Kong
[3]Department of Orthopaedics and Traumatology, The Chinese University of Hong Kong, Shatin, New Territories, Hong Kong
[4]Jockey Club Centre for Osteoporosis Care and Control, The Chinese University of Hong Kong, Shatin, New Territories, Hong Kong
[5]School of Biomedical Sciences, The Chinese University of Hong Kong, Shatin, New Territories, Hong Kong

An innovative anti-osteoporosis herbal formula containing Epimedii Herba, Ligustri Lucidi Fructus and Psoraleae Fructus (ELP) has been previously shown its bone protecting effects in ovariectomized osteoporotic rats and also in post-menopausal osteopenic women. This study aimed to investigate the efficacy of ELP against bone loss during physical inactivity or weightlessness. A hindlimb unloading tail-suspended rat model was used for studying the effects of ELP on bone mineral density (BMD) and bone micro-architecture. For *in vitro* mechanistic studies, rat mesenchymal stem cells (MSCs) and mouse macrophage cells (RAW264.7) were used for studying the effects of ELP on osteogenic/adipogenic differentiations and osteoclastogenesis, respectively. Our data illustrated that ELP had a significant preventive effect against bone loss induced by tail-suspension (TS) at day 28 ($p < 0.01$) as indicated in the reduction in BMD loss and the preservation of bone micro-architecture. ELP could significantly promote the osteogenesis and suppress the adipogenesis ($p < 0.05$) in MSCs. Besides, significant inhibition of osteoclast formation ($p < 0.01$) was found in ELP-treated RAW264.7 cells upon receptor activator of nuclear factor kappa-B ligand induction. Our study presents the first scientific evidence that ELP had a significant preventive effect against bone loss induced by TS through the actions of enhancing osteogenesis, suppressing adipogenesis and osteoclastogenesis.

Keywords: tail-suspension; disuse osteoporosis; Epimedii Herba; Ligustri Lucidi Fructus; Psoraleae Fructus; mesenchymal stem cell; osteogenesis; adipogenesis; osteoclastogenesis.

INTRODUCTION

Disuse osteoporosis is a well-known result of skeletal unloading in humans during long-duration space flight or prolonged bed rest (Lang *et al*., 2004; Watanabe *et al*., 2004) that increases the susceptibility to fractures. It is commonly found in elderly and patients requiring prolonged immobilization or bed rest. A 3.6% and 3.4% reduction of trochanteric and total hip BMD, respectively, was observed after 17 weeks of bed rest (Shackelford *et al*., 2004). *In vivo* studies also demonstrated marked bone loss, disruption of bone architecture and impairment of bone mechanical properties following space flight (Smith *et al*., 1999) or immobilization by tail-suspension (TS) (Ishijima *et al*., 2002; Martin *et al*., 2007). A hindlimb unloading TS model is frequently used in the studies relating to microgravity because it mimics some aspects of exposure to microgravity by eliminating weight-bearing loads from the hindquarters and producing a cephalic fluid shift (Morey-Holton and Globus, 1998).

The Chinese herbal formulation ELP, which contains three 'kidney-tonifying' herbs: Epimedii Herba (E), Ligustri Lucidi Fructus (L) and Psoraleae Fructus (P) with a weight ratio of 5:4:1, has been shown to be prominent in inhibiting the spinal bone mineral density (BMD) loss in aged overiectomized osteoporotic female rats without any adverse side effects (Sun *et al*., 2008). Clinically, ELP also demonstrated its potential benefit in improving BMD on the women who experienced over 10 years of menopause (Leung *et al*., 2011). Recently, there has been increasing evidence indicating the component herbs of ELP can effectively promote the bone health. For instance, it was reported that Epimedii Herba-derived flavonoids could exert anabolic effects on osteoporotic bone from ovariectomized rats by concomitantly promoting osteogenic and suppressing

* Correspondence to: Chun-Hay Ko, E302a, Institute of Chinese Medicine, Science Centre East, The Chinese University of Hong Kong, Shatin, NT, Hong Kong, China. Ping-Chung Leung, Centre for Clinical Trials on Chinese Medicine, 5/F, School of Public Health Building, Prince of Wales Hospital, Shatin, NT, Hong Kong.
E-mails: gohey@cuhk.edu.hk; pingcleung@cuhk.edu.hk

Received 27 December 2011
Revised 13 April 2012
Accepted 02 May 2012

adipogenic differentiation of bone mesenchymal stem cells (MSCs) (Peng *et al*., 2009). This result was similar to our previous finding on the osteoprotective effects of Ligustri Lucidi Fructus aqueous extract in aged ovariectomized rats (Ko *et al*., 2010). Besides, Fructus Psoraleae extract was reported be effective in increasing the bone density and improving the bone architecture *in vivo* (Wong and Rabie, 2010).

Apart from the elevation of osteoclastogenesis, there has been accumulating evidence that the loss of balance between osteogenesis and adipogenesis in MSC differentiation, with adipogenesis predominant over osteogenesis, is another key factor of osteoporosis in human (Gimble *et al*., 2006). MSCs are pluripotent progenitor cells giving rise to osteoblasts, adipocytes, chondrocytes and myocytes. There is a reciprocal relation between the differentiation of adipocytes and osteoblasts (Prockop, 1997). Clinical studies showed an increase in differentiation of MSCs into adipocytes instead of osteoblasts in a variety of osteoporosis (Nuttall and Gimble, 2004). Pan *et al*. reported that TS decreased the expression of osteoblast gene marker mRNAs in MSC, but increased the expression of adipocyte gene markers in rats (Pan *et al*., 2008). Therefore, the enhancement of osteogenesis with a concomitant decrease in adipogenesis may provide a therapeutic target to the treatment of osteoporosis by increasing bone formation through diverting the adipogenesis in MSCs to osteogenesis (Fu *et al*., 2008).

ELP has been shown to significantly prevent bone loss induced by estrogen deficiency. However, there is no direct evidence supporting its inhibitory effect toward bone loss during physical inactivity. Therefore, in the present study, we used the TS rat model to determine the effects of ELP on biological indices of bone metabolism, including BMD and bone micro-architecture during physical inactivity or weightlessness. With regard to the underlying mechanisms in osteoporosis, the *in vitro* cell models of MSC and RAW 264.7 cells were employed to study the osteogenesis/adipogenesis and osteoclastogenesis, respectively, under the treatment of ELP.

MATERIALS AND METHODS

Herbal materials, extraction and standardization. The raw herbs of Epimedii Herba, Ligustri Lucidi Fructus and Psoraleae Fructus were purchased from a local herbal supplier in Hong Kong. The identities of all herbs were authenticated using thin-layer chromatography with reference to methods recommended by the Chinese Pharmacopoeia (Chinese Pharmacopeia Commission, 2010). Herbarium voucher specimens of the tested herbs were deposited at the museum of the Institute of Chinese Medicine, the Chinese University of Hong Kong, with numbers as follows: 2004–2547, 2004–2566, 2004–2568. To prepare the herbal aqueous mixture, the raw herbs were crushed into small pieces and extracted with distilled water twice by heating under reflux. The collected extracts were filtered and lyophilized to give the powder, with the extraction yield of 20%. The content of icariin, psoralen, isopsoralen, oleanolic acid and ursolic acid were quantified by high performance liquid chromatography as 0.081%, 0.017%, 0.014%, 0.004% and 0.006%, respectively (data not shown). The powder was stored in desiccators at room temperature before use.

Animals and treatment protocol. Forty-six male 3-month-old Sprague–Dawley rats (weighing 446.0 ± 38.4 g) were obtained from the Laboratory Animal Services Centre of the Chinese University of Hong Kong. All of them were housed in a temperature and light-controlled environment and were allowed access to standard rodent chow and water *ad libitum* throughout the study. Body weights of the animals were recorded at the beginning and at the end of the study. An animal ethic approval had been obtained from the Animal Experimental Ethics Committee of the Chinese University of Hong Kong (Ref No. 07/052/MIS) for this study.

After seven days of acclimatization, the rats were divided into five groups: TS control (TS), non TS control (Non-TS), TS with high, medium or low dose of ELP (TS-H, TS-M and TS-L, respectively). For Non-TS group, rats were allowed to move freely with their four limbs (without hindlimb unloading). In groups TS (TS-H, TS-M and TS-L), the tails of the rats were suspended so that their hindlimbs were unloaded. Using gastric tube, rats in TS-H received ELP in 2.5 g/day orally while those in TS-M and TS-L received ELP in 1.25 and 0.625 g/day, respectively. The concentration of each drug was adjusted so that each rat was fed with approximately 2.0 ml of drug per day, with little variations depending on its body weight. Rats in both TS and Non-TS received equal volume of distilled water vehicle (2.0 ml/day).

Tail-suspension model. The protocol of the TS was modified from that of Morey-Holton (Morey-Holton and Globus, 1998). Briefly, the tail of each rat was suspended by applying an adhesive tape on its lateral surfaces. Three surgical tapes were then applied circularly at the base, middle and at the end of the region where the adhesive tape contacting the tail in order to secure the adhesion. The loop of the adhesive tape at the tip of the tail passed through a metallic hollow column which was then connected to a 360° free rotating hook via a metallic wire. The hook was hanged on an overhead bar at the middle part of the top of a cage. As a result, the rat was maintained in approximately 35° head-down tilt with its hindlimbs unloaded while its forelimbs could be used for locomotion. The overall suspension period was 28 days.

Peripheral quantitative computed tomography (pQCT). BMD at distal femoral metaphysis and proximal tibial metaphysis of the rat were measured using pQCT (XCT2000, Stratec Medizintechnik GmbH, Germany) at Day 0 (before TS) and Day 28. Quality assurance of measurements had been checked by using the hydroxyapatite cone and standard phantoms prior to the scanning of the rats each time. For the BMD measurement, the rat was first anesthetized using a cocktail of ketamine and xylazine intramuscularly. It was then fixed on a custom-made translucent plastic holder to ensure a repeatable positioning. Right distal femur and proximal tibia were scanned under the built-in Research Mode of the pQCT. The scan speed was 25 mm/s with voxel resolution of 0.2 mm. The analytical parameters for trabecular BMD were set as threshold 280 mg/cm^3, contour mode 1 and peel mode 20. The parameters for

cortical BMD were set as threshold 551 mg/cm^3 and peel mode 2. BMD at three regions of interest (total, trabecular and cortical region) at distal femur and proximal tibia were analyzed separately. Total BMD was the overall BMD of the total cross-sectional area of the bone (including both cortical and trabecular area). The trabecular bone region was defended by setting an inner area to 35% of the total cross-sectional area. Cortical BMD was the average BMD at the outermost area of the bone where the BMD was over 551 mg/cm^3. The mean of percentage differences at Day 28 from baseline (Day 0) within the same group were calculated. Cross-sectional comparisons among TS with other groups were also performed.

Micro-computed tomography (micro-CT). The micro-architecture of the left distal femur was analyzed using a micro-CT (MicroCT 40, Scanco Medical, Switzerland). Briefly, the femur was aligned perpendicularly to the scanning axis. The scanning was conducted at 55 kVp and 144 μA with a resolution of 16 μm per voxel. The trabecular bone within the distal femur was identified with semi-automatically drawn contour at each two-dimensional section. Segmentation parameters were fixed at: Sigma = 0.5, Support = 1.0 and Threshold = 245. The volume of interest (VOI) was determined within 50 continuous slices. The micro-architectural parameters of the VOI were obtained through three dimensional reconstructed images with the image analysis program of the micro-CT workstation. Parameters from direct model (bone volume density (BV/TV), trabecular number (Tb.N), trabecular thickness (Tb.Th) and trabecular plate separation (Tb.Sp)) were analyzed.

Culture and characterization of rat MSCs. Rat MSCs were cultured from the bone of the tibiae and femora of the rats (250 g) by centrifugation as described previously (Dobson *et al*., 1999). Isolated bone marrow cells were resuspended in a growth medium consisting of α-MEM (Life Technologies, USA), 10% fetal bovine serum (Life Technologies, USA) and 1% penicillin/streptomycin (Life Technologies, USA), seeded at a density of 2×10^5/cm^2, and incubated at 37 °C in 95% humidified air and 5% CO_2. On day 7, all non-adherent cells were removed and followed by the medium change twice a week. The monolayer of adherent cells was trypsinized by 0.25% trypsin EDTA when it reached half-confluent and re-seeded at a density of 1×10^4/cm^2 (passage 1, P1). Passage 2 (P2) culture was used for all *in vitro* assays. All adherent P2 cells used in this study were positively expressed CD44 and CD90, and negative in CD11b and CD54.

For the differentiation studies, P2 MSCs were seeded in the six-well plates of 2×10^4/cm^2. After three days, the growth medium was replaced with osteogenic medium (growth medium supplemented with 100 nM dexamethasone, 50 μg/ml ascorbate-2-phosphate and 10 mM β-glycerol phosphate) or adipogenic medium (growth medium supplemented with 1 μM dexamethasone, 50 μg/ml insulin, 0.5 mM methyl-isobutylxanthine and 100 μM indomethacin), with medium changed twice a week. ELP was prepared as stock solution in PBS and sterilized by filtration with 0.22 μm filter. This was then added to both differentiation media to provide final concentrations in the range within 100 μg/ml.

Cell viability assay. The cell viability of undifferentiated MSCs was determined by the 3-[4,5-dimethylthiazol-2-yl]- 2,5-diphenyl-tetrazolium bromide (MTT; Sigma, USA) assay after treatment with ELP aqueous extract (Sigma, USA) at various concentrations in 96-well plates (5×10^3 cells/well) for 5, 10 and 18 days. The relative viable cell viability was determined by measuring the reduction of MTT dye in live cells to blue formazan crystals at optical density at 540 nm and expressed as the percentage of control group without ELP treatment.

Assessment of osteogenic and adipogenic differentiation markers in MSCs. To determine the effect of ELP aqueous extract on osteogenesis in MSCs, we measured the related biochemical markers, namely alkaline phosphatase (ALP) activity and matrix calcium deposition. ALP activity was measured in the cell culture with the commercially available ALP assay kit (Stanbio, USA) after 5 days of osteogenic treatment. Total protein content was determined with BCA protein assay reagent (Sigma, USA) and enzyme activities were expressed as U/mg protein. The matrix calcium deposition was quantified with Stanbio Total LiquiColor calcium determination kit (Stanbio, USA) after 10 days of osteogenic treatment and the readout was normalized by protein content determined by BCA assay reagent (Sigma, USA). The calcification was visualized by staining the cells with 2% Alizarin Red S solution for five minutes after the fixation with 10% buffered formalin (v/v) for 30 min. For adipogenesis, the number of adipocytes was determined with the Oil Red O staining method (Heim *et al*., 2004). After 18 days of ELP treatment in adipogenic medium, the culture cells were rinsed twice with PBS and fixed with 10% buffered formalin (v/v) for 10 min. Fixed cells were washed and stained with 0.2% Oil Red O in 60% isopropanol for 15 min. Excessive stain was removed by 60% isopropanol and then distilled water for three times. Counterstaining for the nucleus was performed with Mayer's hematoxylin for 30 s. Photomicrographs were taken with an inverted microscope at 40× magnification. The number of adipocytes per field was calculated by averaging the counting Oil Red O-positive cells in eight separated views. Approximately, 200 cells were counted in each field and 20% to 30% of total cells were differentiated into adipocytes after 14 days of induction.

Assessment of osteoclast formation and resorption on ELP-treated culture. For the study of osteoclastic differentiation, murine monocyte/macrophage RAW 264.7 cells (ATCC, USA) were seeded in 96-well plates at a density of 1.5×10^4 cells/cm^2 in DMEM (Life Technologies, USA). After 1 day of incubation, the differentiation of osteoclasts from RAW 264.7 cells was induced with 50 ng/mL of recombinant mouse soluble RANKL (Sigma, USA) in α-MEM (Life Technologies, USA) with 10% FBS for 3 days. After treatment with RANKL and different concentrations of ELP for 3 days, the RAW 264.7 cell differentiated osteoclasts were fixed and stained for tartrate-resistant acid phosphatase (TRAP), an osteoclast enzyme marker, by using an acid phosphatase kit (Sigma, USA) according to the manufacturer's instructions. TRAP-positive multinucleated cells showing more than three nuclei were counted as osteoclasts. Photomicrographs were taken with an inverted microscope at 40× magnification. The number

of osteoclasts per field was calculated by averaging the counting from eight separated views. Meanwhile, the cell viability was also tested on undifferentiated cells for 3 days using MTT method. For dentine resorption assay, the RAW 264.7 cells were seeded on dentine slices (IDS, UK) that had been placed in 96-well plates, which were then further incubated in the presence of RANKL and different concentrations of ELP for 7 days. After incubation, attached cells were completely removed from the dentine slices by 0.1 N sodium hydroxide under sonification. Resorption pits on the slices were observed using 1.0% (v/v) toluidine blue staining under reflected microscopy. The number of resorption pits per dentine slice was quantified. For mRNA analysis, the cells were seeded on 6-well plate at a density of 1.5×10^4 cells/cm^2. Total mRNA of each treated osteoclastic culture was also isolated by the RNeasy mini kit (Qiagen, USA) and stored at $-20\,^{\circ}$C. The amount of TRAP mRNA was determined using Quanti-Fast SYBR Green RT-PCR kit (Qiagen, GmbH) with a validated primer set specific for TRAP mRNA (Qiagen, USA; NM_001102404) on the CFX96 real-time PCR detection system (Bio-Rad, USA). The threshold cycle (Ct), the cycle number at which the amount of amplified gene of interest reached a fixed threshold, was determined. Relative expression of the RT-PCR product was calculated using the comparative $2^{-\Delta\Delta Ct}$ method. Endogenous control glyceraldehyde-3-phosphate dehydrogenase mRNA was used for normalization. Fold difference was then determined by normalizing all values to the mean of the relative expression for the control group without treatment.

Statistical analysis. Differences between treatment and control groups (not exposed to ELP extracts) were tested by one-way ANOVA, followed by *post hoc* Dunn's test. All statistical analyses were performed with the Statistical Package of Social Science (SPSS) version 15.0 (SPSS, USA). All statistical tests were carried out at the 5% level of significance ($p < 0.05$). Data were expressed as mean ± standard derivation (SD).

RESULTS

All animal experienced 28-day TS resulted in significant BMD loss when compared with their baseline value at day 0 ($p < 0.001$). No significant weight difference was found between all TS groups before and after the 28 days of experiment (data not shown). Results of the effect of ELP on the change of BMD at distal femur and proximal tibia in TS rats were shown in Table 1. TS caused a significant lower BMD ($p < 0.05$) in both distal femur and proximal tibia when compared with non-tail-suspended group (Non-TS) after 28 days. A more deteriorative effect toward the BMD in trabecular bone (−24.5% and −29.7% in femur and tibia, respectively) than cortical bone (−2.3% and −3.5% in femur and tibia, respectively) after 28-day TS was observed. When the comparison was focused within the tail-suspended groups, decreasing trends in percentage loss of BMD along with increasing of ELP dosage for the trabecular and the total region in both femur (From TS-L to TS-H: decreased from −17.4% to −15.9% in trabecular region; from −9.2% to −7.7% in total region) and tibia (From TS-L to TS-H: decreased from −23.5% to −13.7% in trabecular region; from −8.03% to −7.8% in total region) were found. Thus, ELP exhibited a significant preventive effect against BMD loss in a dose-dependent manner. However, this dose-dependent effect was not shown in cortical bone; it may presumably be due to the overall deteriorate effect on cortical under suspension is minimal. According to the results, the osteoprotective effects of ELP in femur was more pronounced than in tibia, as indicated by the significant difference of BMD loss in the trabecular and cortical regions between TS and the groups treated with ELP.

Summary of bone micro-architectural results for the effects of ELP on TS rat model was shown in Table 2. By comparing with Non-TS, significant lower bone volume fraction (BV/TV) (−27.3%, $p < 0.05$) and trabecular thickness (Tb. Th) (−17.6%, $p < 0.05$) were observed in TS, whereas a significant higher value on trabecular separation (Tb.Sp) (12.0%, $p < 0.05$) was found. In addition, a slight but insignificant increase in (BV/TV), trabecular number (Tb. N) and (Tb. Th) along with increasing ELP dosage within the tail-suspended groups was noted. All the micro-architectural parameters were improved significantly in TS-H when compared with TS ($p < 0.05$). This indicated a dose-dependent effect of ELP on prevention of bone micro-architecture deterioration during TS.

To determine whether ELP could stimulate osteogenic differentiation, the effect of ELP on bone formation marker, ALP activity, was studied. Our data illustrated that treatment of MSCs with ELP for 5 days stimulated ALP activity in a dose-dependent manner

Table 1. Percentage loss of bone mineral density in different region of interest within different groups of rats after 28-day tail-suspension

		TS	TS-L	TS-M	TS-H	Non-TS
Femur	***Trabecular***	−24.46 ± 5.8	−17.41 ± 6.9	−16.51 ± 5.2	−15.93 ± 4.7	2.46 ± 7. 40
	(%)		($p = 0.046$)	($p = 0.016$)	($p = 0.004$)	($p < 0.001$)
	Cortical	−2.32 ± 1.34	−0.578 ± 0.8	−0.676 ± 0.8	−0.29 ± 1.3	3.29 ± 2.08
	(%)		($p = 0.015$)	($p = 0.037$)	($p = 0.002$)	($p < 0.001$)
	Total	−13.18 ± 4.0	−9.18 ± 4.2	−8.42 ± 2.4	−7.73 ± 2.7	3.02 ± 4.83
	(%)			($p = 0.024$)	($p = 0.003$)	($p < 0.001$)
Tibia	***Trabecular***	−29.72 ± 10.0	−23.52 ± 10.8	−17.36 ± 11.6	−13.69 ± 10.1	−2.76 ± 17.9
	(%)				($p = 0.01$)	($p < 0.001$)
	Cortical	−3.48 ± 2.6	1.74 ± 2.6	−0.51 ± 3.7	−0.71 ± 2.2	6.07 ± 2.8
	(%)		($p = 0.003$)			($p < 0.001$)
	Total	−15.05 ± 2.0	−8.03 ± 4.3	−8.02 ± 6.1	−7.83 ± 4.7	5.08 ± 6.7
	(%)		($p = 0.009$)	($p = 0.009$)	($p = 0.005$)	($p < 0.001$)

Results are means ± SD, n = 8–11 rats per group ***(p value indicated a significant difference versus TS; #: p < 0.05 versus TS)***

(Fig. 1a). At 100 μg/mL, the ALP activity was significantly increased by about 1.5 folds ($p < 0.001$) when compared with the respective control without treatment. Besides, the effect of ELP in osteogenic differentiation as evidence by extracellular matrix mineralization was also investigated (Fig. 1b). At 100 μg/ml, ELP significantly increased the matrix calcium deposition by about three folds ($P < 0.001$) after 10 days of incubation. A dose-dependent response of calcium deposition was also observed at lower concentrations of ELP. ELP did not exert cytotoxic effects on the cells as assessed by MTT assay after 5 and 10 days of incubation (Fig. 1c). To investigate the effect of ELP on adipogenic differentiation in rat MSCs, Oil Red O staining was used to visualize the formation of adipocytes after 18 days of adipogenic induction. As shown in Fig. 2a, ELP significantly inhibited the formation of adipocytes in a dose-dependent manner. At 100 μg/mL of ELP, the number of adipocyte was decreased by 88.9% ($p < 0.001$). Our MTT data (Fig. 2b) illustrated that all test dosages of ELP were non-cytotoxic effects to MSCs throughout the differentiation period up to 18 days.

To determine the effects of ELP on RANKL-induced osteoclastogenesis of RAW 264.7 cells, TRAP-positive cells were stained and counted after 3 days of treatment. A dose-dependent inhibitory response (200–400 μg/ml) was observed when compared with non-ELP treated cells with RANKL induction (0 μg/ml). At 400 μg/ml, the number of TRAP-positive osteoclasts was decreased significantly by 74.5% when treated with ELP. Similar findings were found in our real-time RT-PCR analysis, which indicated that ELP could effectively down-regulate TRAP mRNA expression in a dose-dependent manner (100–400 μg/ml) after 3 days of treatment (Fig. 3b). In addition, at 400 μg/ml of ELP, the number of resorption pits formed on dentine slice after 7 days of treatment was also decreased by 50% ($P < 0.001$), which provided a solid evidence to substantiate the anti-osteoclastic effects of this formula (Fig. 3c). Furthermore, our data also demonstrated that the viability of osteoclast precursor RAW 264.7 cells was not affected by ELP with concentrations up to 400 μg/ml (Fig. 3c). Our data indicated that ELP could effectively regulate RANKL-induced osteoclastogenesis on RAW 264.7 cells.

DISCUSSION

In this study, TS rat model was successfully utilized to investigate the impact of ELP on bone deterioration during hindlimb unloading in our laboratory. This study using 3-month-old male rats demonstrated that TS caused detrimental effect on both BMD and trabecular micro-architecture. These findings were in agreement with that reported by Bloomfield *et al.* (Bloomfield *et al.*, 2002). They reported that femoral trabecular bone micro-architecture was markedly deteriorated after hindlimb immobilization. A significant decrease in trabecular BMD, BV/TV and Tb.N was found in tail-suspended rats, paralleled by an increase in trabecular Tb.Sp when compared with the control group without TS. We also found that TS produced a more damaging effect in BMD loss of trabecular structure than cortical part, which was consistent with the report of Habold *et al.* (Habold *et al.*, 2001).

Based on the bone protective effect of ELP in ovariectomy-induced osteoporotic rats (Sun *et al.*, 2008), the present study was designed to provide direct evidence supporting inhibitory effect of ELP toward bone loss during physical inactivity. The current study demonstrated the beneficial effects of ELP in preserving BMD in both trabecular and cortical bone compartments in unloaded hind limbs of TS rats, via oral administration. In particular, ELP significantly reduced total, cortical and trabecular BMD loss in femur in dose-dependent manner after 28-day TS. Similar but less obvious osteoprotective effect of ELP was also found in tibia. The more obvious deteriorative effect toward the BMD in trabecular bone than in cortical bone revealed that there are compartment-specific differences in skeletal response to hindlimb unloading. The major impact of unloading is on cancellous bone sites. These differences had been reported by Bloomfield and her colleagues in their skeletal mature rats (Bloomfield *et al.*, 2002).

Although BMD has been long regarded as a surrogate measure of bone strength, micro-architectural properties provide more comprehensive information to evaluate the impact of ELP on the quality of trabecular bone. In this study, micro-CT analysis indicated that ELP protected the bone micro-architecture against deterioration in femur. The diminished reduction of Tb.N and Tb.Th in TS-H reflected that ELP showed an inhibitory effect against bone resorption during TS and resulted in a higher BV/TV when compared with TS. The preservation of trabecular bone micro-architecture significantly contributed to bone strength, as demonstrated by a number of studies that have been reported close correlations between micro-structural properties and the biomechanical strength of the bone (Teo *et al.*, 2006; Wu *et al.*, 2008; Leahy *et al.*, 2010).

Table 2. Trabecular micro-architectural parameters of distal femoral metaphysis

	TS	TS-L	TS-M	TS-H	Non-TS
BV/TV (%)	0.24 ± 0.03	0.27 ± 0.02 ($p = 0.048$)	0.28 ± 0.03 ($p = 0.039$)	0.29 ±0.02 ($p = 0.001$)	0.33 ± 0.03 ($p < 0.001$)
Tb.N (/mm)	3.45 ± 0.1	3.54 ± 0.2	3.59 ± 0.1	3.73 ± 0.2 ($p = 0.024$)	3.76 ± 0.2 ($p < 0.001$)
Tb.Th (mm)	0.084 ± 0.01	0.092 ± 0.01 ($p = 0.028$)	0.093 ± 0.01 ($p = 0.011$)	0.094 ± 0.01 ($p = 0.003$)	0.102 ± 0.01 ($p < 0.001$)
Tb.Sp (mm)	0.28 ± 0.02	0.27 ± 0.02	0.26 ± 0.01	0.25 ± 0.01 ($p = 0.02$)	0.25 ± 0.02 ($p < 0.001$)

Results are means ± SD, n = 8–11 rats per group ***(p value indicated a significant difference versus TS)***

BV/TV, trabecular bone volume fraction; Tb.N, trabecular number; Tb.Th, trabecular thickness; Tb.Sp, trabecular separation.

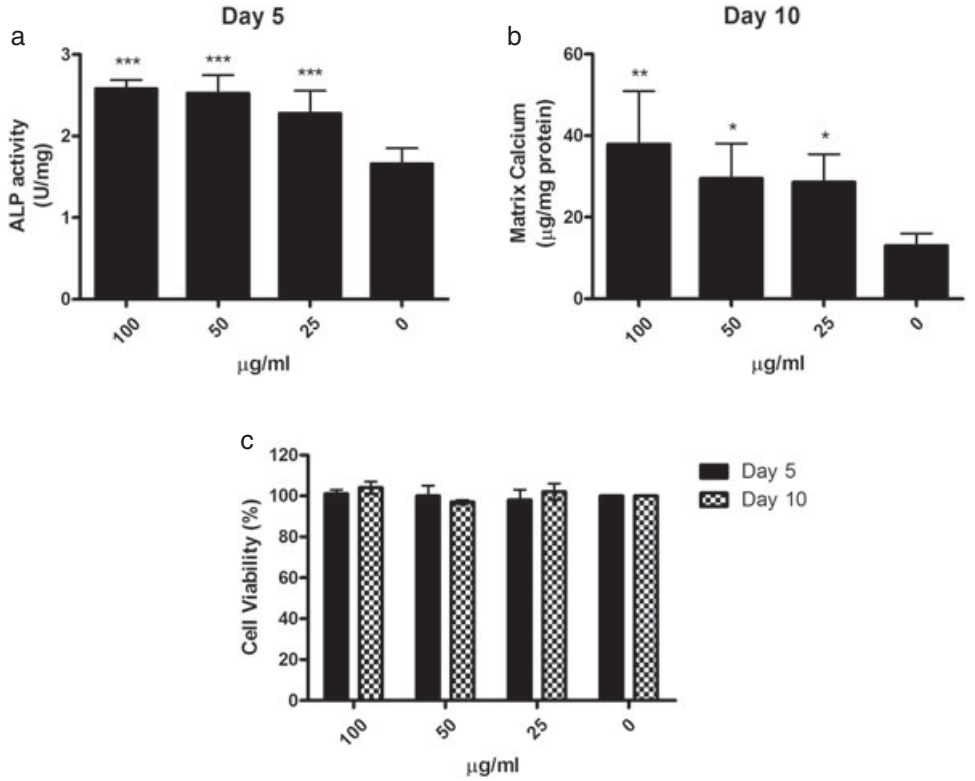

Figure 1. Osteogenic properties of ELP in rat MSCs. Dose effect of ELP on (a) alkaline phosphatase (ALP) activity and (b) extracellular matrix calcium content in MSCs were determined under osteogenic induction on day 5 and day 10, respectively. (c) Effect of ELP on the cell viability of undifferentiated rat MSCs. MSCs were treated with different concentrations of ELP for 5 and 10 days. The cell viability was estimated by MTT assay. Data are the mean ± SD (n = 3) from three independent experiments. Significant difference: * $p < 0.05$; ** $p < 0.01$; *** $p < 0.001$ for difference from respective baseline cultures without treatment.

Recently, it has been reported that TS reduced the proliferation and differentiation of putative osteoblast precursor MSCs (Pan *et al.*, 2008). It was also found that the number and volume of adipocytes in the bone marrow stroma were increased in tail-suspended rats (Ahdjoudj *et al.*, 2002). These observations suggested that increased adipogenesis of MSCs of osteoporotic individuals was coupled with decreased osteogenic potential. Modulation of differentiation of MSCs towards the osteogenic from adipogenic lineage would promote overall bone formation and could be used as a novel therapeutic strategy in disuse osteoporosis. In the present study, we demonstrated that ELP significantly increased the bone formation in rat osteoprogenitor MSCs. This was indicated by the dose-dependent increase in bone marker, ALP activities and extracellular matrix mineralization, upon the addition of ELP to the MSCs in osteogenic medium, without cytotoxic effects. Despite these pro-osteogenic effects in MSCs, ELP also inhibited adipogenesis as indicated by the decrease of adipocytes numbers.

Skeletal unloading not only suppresses osteoblastic activities, but also enhances osteoclastic activities in the bone (Saxena *et al.*, 2011). Histomorphometric

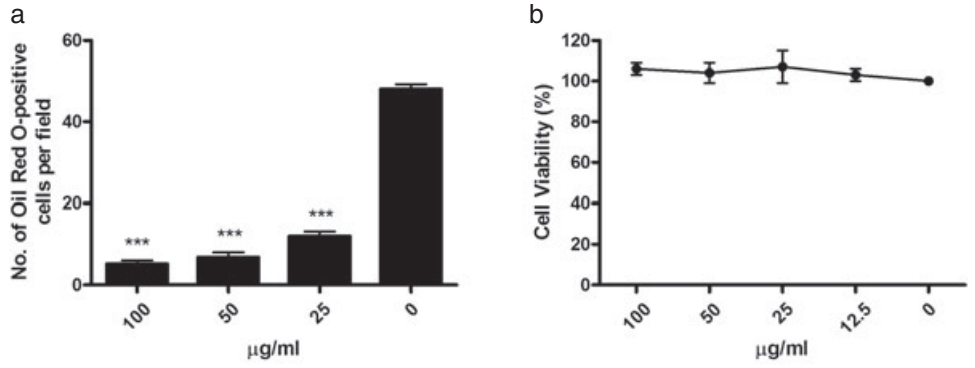

Figure 2. Anti-adipogenic properties of ELP in rat MSCs. (a) The number of adipocytes per field was counted after Oil-red O staining on day 18. The number of adipocytes per field was calculated by averaging the counting from eight separated views (Magnification: 40×). (b) Effect of ELP on the cell viability of undifferentiated rat MSCs. MSCs were treated with different concentrations of ELP for 18 days. The cell viability was estimated by MTT assay. All results are expressed as mean ± SD of three independent experiments. Significant difference: * $p < 0.05$; ** $p < 0.01$; *** $p < 0.001$ for difference from respective baseline cultures without treatment.

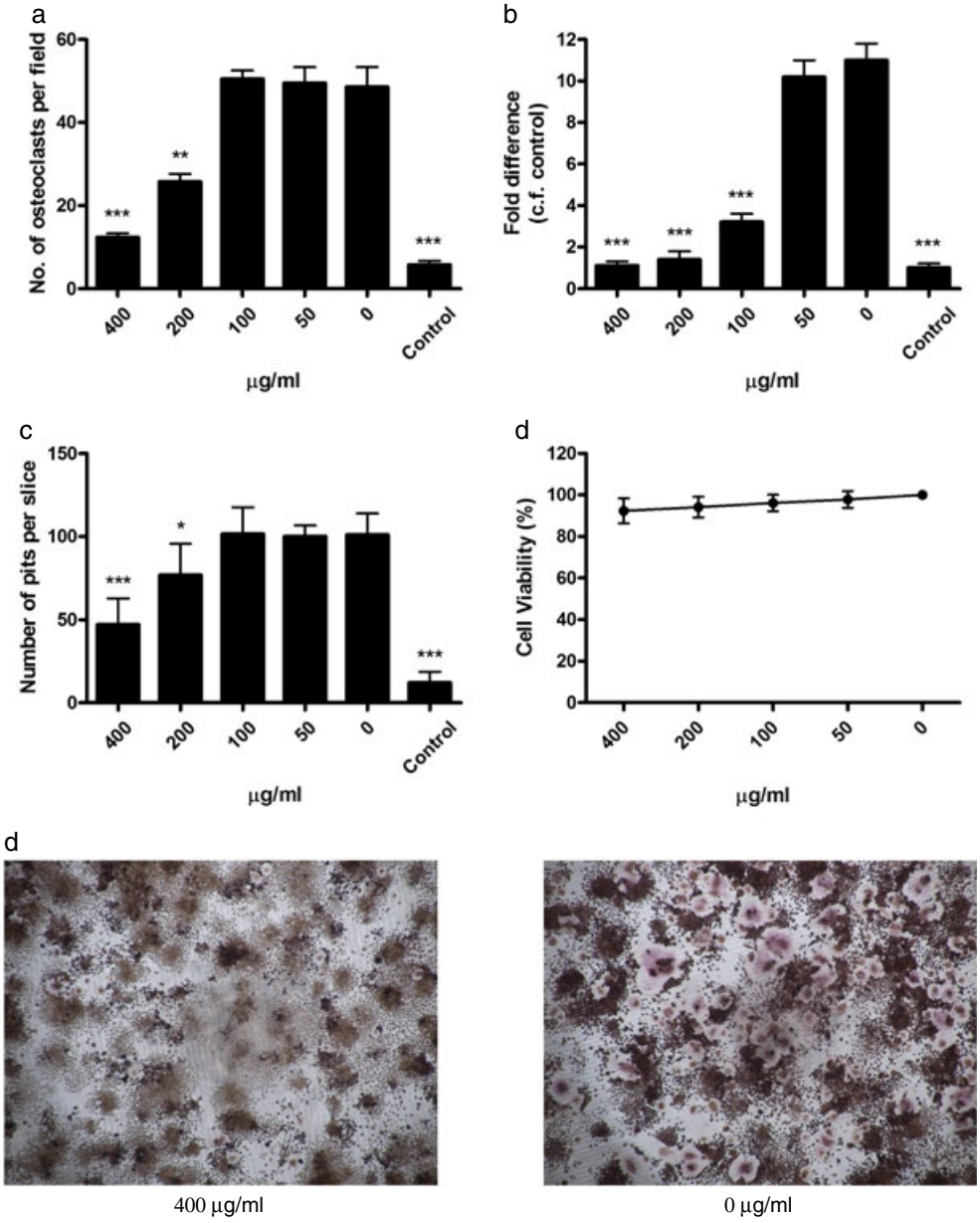

Figure 3. Anti-osteoclastogenic properties of ELP in RAW264.7 cells upon RANKL induction. (a) The number of osteoclasts was counted after 3 days of ELP treatment. TRAP-positive multinucleated cells with more than three nuclei were considered as osteoclasts. The number of osteoclasts per field was calculated by averaging the counting from eight separated views (Magnification: 40×). (b) Inhibitory effect of ELP on TRAP mRNA expression of RAW 264.7 cells upon RANKL induction for 3 days. The expression level of TRAP gene was normalized on the basis of GAPDH expression. Fold difference was determined as the relative expression, compared with cells without ELP treatment. (c) The number of resorption pits per dentine slice was counted after 7 days of ELP treatment. (d) Effect of ELP on the cell viability of undifferentiated RAW264.7 cells. RAW264.7 cells were treated with different concentrations of ELP for 3 days, and the cell viability was estimated by MTT assay. All results are expressed as mean ± SD of three independent experiments each in triplicates. Significant difference: * $p < 0.05$; ** $p < 0.01$; *** $p < 0.001$ for difference from respective baseline cultures without treatment. (e) Osteoclast formation was effectively inhibited by ELP at 400 μg/mL ELP when compared with control group without treatment (Magnification: 40×).

investigations of rats in spaceflight showed an increase in the number of osteoclasts, and osteoclast-mediated mineral resorption was enhanced (Földes *et al*., 1990; Vico *et al*., 1993). Our results showed that exposure of osteoclast precursors RAW264.7 to ELP inhibited their sensitivity to RANKL which stimulates them to form giant multinucleated osteoclasts and decrease in osteoclastogenesis markers TRAP mRNA expression. Also, ELP decreased the osteoclastic bone resorption activities. ELP may protect the bone in TS rat model by its anti-osteoclastic nature. To date, interventions for preventing TS-induced bone loss have mainly used bisphosphonates that suppress resorption (Mosekilde *et al*., 2000). For instance, Lloyd *et al*. have showed that the use of a low-dose bisphosphonate, zolendronic acid in conjunction with osteoprotegerin counteracted BMD loss occurring in mice due to 28 days of hindlimb unloading (Lloyd *et al*., 2008).

In the theory of Chinese medicine, different combinations of herbs can cause systemic therapeutic effects in human subjects. Apart from their individual bioactivities, the herbs may contain various components that act synergistically to reinforce the bioactivities of others, thereby modulating the therapeutic effects of the herbal

medicine (Li *et al*., 2008). However, the specific interactions between E, L and P in ELP need to be determined in the future. Future work will focus on the interaction between different ELP components responding to the underlying mechanisms. Furthermore, their interaction with commonly used anti-resorptive, such as bisphonsphonates and raloxifene, will be studied also in order to determine the safety profile and possible herb-drug synergistic effects for osteopenic human subjects.

In conclusion, the present study provides the first evidence to the *in vivo* efficacy of using ELP in ameliorating bone deterioration induced by TS. Moreover, our *in vitro* data demonstrated that the bone protective effects of ELP might be due to its direct influence on bone formation and inhibition of adipocyte and osteoclast formation. These speculations will be further confirmed by inclusion of histomorphometric data which would have identified the cellular mechanism of action - i.e. up- or down-regulation of osteoblasts or osteoclasts. This study has proven that the three herbs formula ELP has strong support from Chinese Medicine Classics as good agents for the maintenance of bone health. Now that more and more adverse effects on long-term administration of potent anti-resorptive pharmaceuticals have been reporting. Hence, they might be suitable only for those suffering from severe osteoporosis, when there is immediate threat to fractures. ELP can be developed as an alternative supplement to maintain a good balance between bone formation and resorption. It could be a timely offer for those who suffer from disuse osteoporosis because of prolonged immobilization or bed rest, as a preventive intervention.

Acknowledgement

This study was supported by the Ming Lai Foundation, The International Association of Lions Clubs District 303 and Hong Kong & Macau Tam Wah Ching Chinese Medicine Resource Centre.

Conflict of Interest

The authors have declared that there is no conflict of interest.

REFERENCES

Ahdjoudj S, Lasmoles F, Holy X, Zerath E, Marie PJ. 2002. Transforming growth factor beta2 inhibits adipocyte differentiation induced by skeletal unloading in rat bone marrow stroma. *J Bone Miner Res* **17**: 668–677.

Bloomfield SA, Allen MR, Hogan HA, Delp MD. 2002. Site- and compartment-specific changes in bone with hindlimb unloading in mature adult rats. *Bone* **31**: 149–157.

Chinese Pharmacopeia Commission. 2010 *Chinese Pharmacopeia Commission, Pharmacopoeia of the People's Republic of China*. Chinese Medical Science and Technology Press: Beijing, China.

Dobson KR, Reading L, Haberey M, Marine X, Scutt A. 1999. Centrifugal isolation of bone marrow from bone: an improved method for the recovery and quantitation of bone marrow osteoprogenitor cells from rat tibiae and femurae. *Calcif Tissue Int* **65**: 411–413.

Földes I, Rapcsák M, Szilágyi T, Oganov VS. 1990. Effects of space flight on bone formation and resorption. *Acta Physiol Hung* **75**: 271–285.

Fu L, Tang T, Miao Y, Zhang S, Qu Z, Dai K. 2008. Stimulation of osteogenic differentiation and inhibition of adipogenic differentiation in bone marrow stromal cells by alendronate via ERK and JNK activation. *Bone* **43**: 40–47.

Gimble JM, Zvonic S, Floyd ZE, Kassem M, Nuttall ME. 2006. Playing with bone and fat. *J Cell Biochem* **98**: 251–266.

Habold C, Momken I, Ouadi A, Bekaert V, Brasse D. 2001. Effect of prior treatment with resveratrol on density and structure of rat long bones under tail-suspension. *J Bone Miner Metab* **29**: 15–22.

Heim M, Frank O, Kampmann G, *et al*. 2004. The phytoestrogen genistein enhances osteogenesis and represses adipogenic differentiation of human primary bone marrow stromal cells. *Endocrinology* **145**: 848–859.

Ishijima M, Tsuji K, Rittling SR, *et al*. 2002. Resistance to unloading-induced three-dimensional bone loss in osteopontin-deficient mice. *J Bone Miner Res* **17**: 661–667.

Ko CH, Siu WS, Lau CP, Lau CB, Fung KP, Leung PC. 2010. Osteoprotective effects of Fructus Ligustri Lucidi aqueous extract in aged ovariectomized rats. *Chin Med* **5**: 39.

Lang T, LeBlanc A, Evans H, Lu Y, Genant H, Yu A. 2004. Cortical and trabecular bone mineral loss from the spine and hip in long-duration spaceflight. *J Bone Miner Res* **19**: 1006–1012.

Leahy PD, Smith BS, Easton KL, *et al*. 2010. Correlation of mechanical properties within the equine third metacarpal with trabecular bending and multi-density micro-computed tomography data. *Bone* **46**: 1108–1113.

Leung PC, Cheng KF, Chan YH. 2011. An innovative herbal product for the prevention of osteoporosis. *Chin J Integr Med* **17**:744–749.

Li S, Han Q, Qiao C, Song J, Lung CC, Xu H. 2008. Chemical markers for the quality control of herbal medicines: an overview. *Chin Med* **3**: 7.

Lloyd SA, Travis ND, Lu T, Bateman TA. 2008. Development of a low-dose anti-resorptive drug regimen reveals synergistic suppression of bone formation when coupled with disuse. *J Appl Physiol* **104**: 729–738.

Martin A, David V, Malaval L, Lafage-Proust MH, Vico L, Thomas T. 2007. Opposite effects of leptin on bone metabolism: a dose-dependent balance related to energy intake and insulin-like growth factor-I pathway. *Endocrinology* **148**: 3419–3425.

Mosekilde L, Thomsen JS, Mackey MS, Phipps RJ. 2000. Treatment with risedronate or alendronate prevents hind-limb immobilization-induced loss of bone density and strength in adult female rats. *Bone* **27**: 639–645.

Morey-Holton ER, Globus RK. 1998. Hindlimb unloading of growing rats: a model for predicting skeletal changes during space flight. *Bone* **22**: 83S-88S.

Nuttall ME, Gimble JM. 2004. Controlling the balance between osteoblastogenesis and adipogenesis and the consequent therapeutic implications. *Curr Opin Pharmacol* **4**: 290–294.

Pan Z, Yang J, Guo C, *et al*. 2008. Effects of hindlimb unloading on ex vivo growth and osteogenic/adipogenic potentials of bone marrow-derived mesenchymal stem cells in rats. *Stem Cells Dev* **17**: 795–804.

Peng S, Zhang G, He Y, *et al*. 2009. Epimedium-derived flavonoids promote osteoblastogenesis and suppress adipogenesis in bone marrow stromal cells while exerting an anabolic effect on osteoporotic bone. *Bone* **45**: 534–544.

Prockop DJ. 1997. Marrow stromal cells as stem cells for nonhematopoietic tissues. *Science* **276**: 71–74.

Saxena R, Pan G, Dohm ED, McDonald JM. 2011. Modeled microgravity and hindlimb unloading sensitize osteoclast precursors to RANKL-mediated osteoclastogenesis. *J Bone Miner Metab* **29**: 111–122.

Shackelford LC, LeBlanc AD, Driscoll TB, *et al*. 2004. Resistance exercise as a countermeasure to disuse-induced bone loss. *J Appl Physiol* **97**: 119–129.

Smith SM, Wastney ME, Morukov BV, *et al*. 1999. Calcium metabolism before, during, and after a 3-mo spaceflight: kinetic and biochemical changes. *Am J Physiol* **277**: R1–R10.

Sun Y, Lee SM, Wong YM, *et al*. 2008. Dosing effects of an antiosteoporosis herbal formula--a preclinical investigation using a rat model. *Phytother Res* **22**: 267–273.

Vico L, Bourrin S, Genty C, Palle S, Alexandre C. 1993. Histomorphometric analyses of cancellous bone from COSMOS 2044 rats. *J Appl Physiol* **75**: 2203–2208.

Watanabe Y, Ohshima H, Mizuno K, *et al*. 2004. Intravenous pamidronate prevents femoral bone loss and renal stone formation during 90-day bed rest. *J Bone Miner Res* **19**: 1771–1778.

Wong RW, Rabie AB. 2010. Systemic effect of Fructus Psoraleae extract on bone in mice. *Phytother Res* **24**: 1578–1580.

Teo JC, Si-Hoe KM, Keh JE, Teoh SH. 2006. Relationship between CT intensity, micro-architecture and mechanical properties of porcine vertebral cancellous bone. *Clin Biomech (Bristol, Avon)*. **21**: 235–244.

Wu ZX, Lei W, Hu YY, *et al*. 2008. Effect of ovariectomy on BMD, micro-architecture and biomechanics of cortical and cancellous bones in a sheep model. *Med Eng Phys* **30**: 1112–1118.

